Paper 12

©Civil-Comp Press, 2012
Proceedings of the Eleventh International Conference
on Computational Structures Technology,
B.H.V. Topping, (Editor),
Civil-Comp Press, Stirlingshire, Scotland

The Torsion Effects on the Non-Linear Behaviour of Thin-Walled Beams: A Finite Element Approach

F. Mohri[1], N. Damil[2] and M. Potier-Ferry[1]
[1]LEM3, CNRS UMR 7239, University of Lorraine, Metz, France
[2]LCSM, Faculty of Sciences Ben M'Sik
University Hassan II, Casablanca, Morocco

Abstract

The authors have developed a beam finite element model for thin walled beams with arbitrary cross sections in the large torsion context [1]. Circular functions of the torsion angle θ_x ($\boldsymbol{c}=\cos\theta_x-1$ and $\boldsymbol{s}=\sin\theta_x$) were included as variables. In this paper three other three-dimensional finite element beams are derived according to the three approximations of the circular functions c and s: cubic, quadratic and linear. A finite element approach of these approximations is carried out. Many comparison examples are considered. They concern non linear behaviour of beams under twist moment and post buckling behaviour of beams under axial loads or bending loads.

Keywords: beam, finite element, non linear, open section, post-buckling, stability, thin-walled.

1 Introduction

Thin-walled elements with isotropic or anisotropic composite materials are extensively used as beams and columns in engineering applications, ranging from buildings to aerospace and many other industry fields where requirements of weight saving are of main importance. Due to their particular shapes resulting from the fabrication process, these structures always have open sections that make them highly sensitive to torsion, instabilities and to imperfections. The instabilities are then the most important phenomena that must be accounted for in design. Nevertheless most of these flexible structures can undergo large displacements and deformations without exceeding their yield limit. Again, buckling does not mean failure. Many structures depict a stable equilibrium in post buckling state. For these reasons the computation of these structures must be carried out according to nonlinear models with use of an efficient technique that is able to overcome the difficulties encountered in presence of singular points.

In literature of thin-walled beams, some finite element models were derived from Vlasov's model in small non-uniform torsion context [2],[3]. Pi [4] and Turkalj [5] introduced a correction in the rotation matrix by considering higher order terms and obtained improved models for linear and nonlinear stability analyses. Moreover, it has been proved that pre-buckling deformations and shortening effects have a predominant influence on torsion behaviour and stability of thin-walled beams especially in beam lateral buckling investigations. These phenomena result from flexural torsional coupling and presence of cubic term in the torsion equilibrium equation (shortening effect or Wagner's terms). These parameters are naturally ignored in models developed according to linear stability. Authors [1] have developed a beam finite element model for thin-walled beams with arbitrary cross sections including flexural-torsional coupling, pre-buckling deflection effects and large torsion context (B3Dw element). The efficiency of the model has been proved for nonlinear behaviour and post buckling behaviour of thin-walled beams with arbitrary cross sections. Comparisons have been made with some available beam finite element with co-rotational formulation or test results.

Furthermore, some other finite element models have been investigated for stability of thin-walled beams where the trigonometric functions were approximated by polynomial functions. A finite element approach with cubic approximation was investigated by Attard [6] and Ronagh [7]. In these works, only results on stability were reported. Mohri [8] adopted this approximation in presence of cubic curvature and developed a semi analytical model for post buckling behaviour of simply supported beams when buckling modes are sinusoidal. Dourakopoulos [9] adopted the same approximation with boundary element method. DeVille [10] investigated a beam finite element with co-rotational formulation and linear approximation of circular functions. Similar approximations were obtained in Fraternali [11] with an additional higher term for warping component.

Nonlinear behaviour of structures like beam is conditioned by many parameters (mesh, geometry data, boundary conditions, initial imperfections, iterative method and convergence criteria). It is important to discuss the effect of different approximations under the same conditions. In the present original work, a finite element formulation is derived according to each approximation (cubic element, quadratic and linear approximation). For each element, flexural-torsional coupling is taken into account in kinematics (displacement and Green's tensor components) and the equilibrium in Lagrangian assumption. In solution the incremental iterative methods are followed. The tangent stiffness matrix of each approximation is carried out. Each element is incorporated in a homemade finite element code. Many comparison examples are considered. They concern non linear behaviour of beams with arbitrary cross section under twist moment and post buckling behaviour of columns and beams. For each element, the flexural-torsional equilibrium paths are obtained under the same conditions. The efficiency of B3Dw element is confirmed.

The background of the large torsion model is first reminded in section 2. The equilibrium and the constitutive equations are first described in section 2.1. The finite element discretisation, tangent matrix terms and the solution strategy follow in section 2.2. In section 3, the finite element formulation according to cubic approximation is described and followed by quadratic and linear approximations. The main changes are outlined.

2 Theoretical and numerical model background

2.1 Equilibrium and constitutive equations

The theoretical model used in this work has been detailed in [1]. For the sake of completeness, only a short review is shown hereafter and attention is gone to model parts where flexural torsion coupling exist and torsion approximation is present. For the study, a straight thin-walled element with slenderness L and an open cross-section A is pictured in Fig. 1. A direct rectangular co-ordinate system (x,y,z) is chosen. Origin of these axes is located at the centre G and shear centre is denoted by C. Consider M, a point on the section contour with its co-ordinates (y, z, ω), ω being the sectorial co-ordinate introduced in Vlasov's model for non uniform torsion. It is admitted that there is no shear deformations in the mean surface of the section and the contour of the cross-section is rigid in its own plane. Displacements and twist angle can be large but deformations are assured to be small. An elastic behaviour is then adopted in material behaviour. Displacements of a point M are derived from those of the shear centre by:

$$u_M = u - y(v' + v'c + w's) - z(w' + w'c - v's) - \omega\theta_x' \tag{1}$$

$$v_M = v - (z - z_c)s + (y - y_c)c \tag{2}$$

$$w_M = w + (y - y_c)s + (z - z_c)c \tag{3}$$

with $c = \cos(\theta_x) - 1$ and $s = \sin(\theta_x)$ (4a,b)

u is the axial displacement of centroid, (v, w) are displacements of shear point in y and z directions and θ_x is the torsion angle. Customary symbol (.)' denotes differentiation with respect to x co-ordiante. Since the model is concerned with large torsion, the trigonometric functions c and s are conserved without any approximation in this section. The components of Green's strain tensor which incorporate large displacements are reduced to the following:

$$\varepsilon_{xx} = \varepsilon - yk_z - zk_y - \omega\theta_x'' + \frac{1}{2}R^2\theta_x'^2 \tag{5a}$$

$$\varepsilon_{xy} = -\frac{1}{2}\left(z - z_c + \frac{\partial\omega}{\partial y}\right)\theta_x' \qquad \varepsilon_{xz} = \frac{1}{2}\left(y - y_c - \frac{\partial\omega}{\partial z}\right)\theta_x' \tag{5b,c}$$

In (5a), ε denotes the membrane component, k_y and k_z are beam curvatures about the main bending axes and R is the distance between the point M and the shear centre C. One reads:

$$\varepsilon = u' + \frac{1}{2}(v'^2 + w'^2) - \chi\theta'_x$$
$$k_y = w'' + w''c - v''s$$
$$k_z = v'' + v''c + w''s \qquad (6a,c)$$

The variable χ associated with membrane component in (6a) is defined by:

$$\chi = y_c(w' + w'c - v's) - z_c(v' + v'c + w's) \qquad (6d)$$

Equilibrium equations are derived from stationary conditions of the total potential energy (δU-δW=0). Loads are applied on the external surface of the beam ∂A (Fig.1). Their components ($\lambda F_{xe}, \lambda F_{ye}, \lambda F_{ze}$) are supposed to be proportional to load parameter λ. The beam strain energy δU is written in terms of the stress resultants acting on the cross-section as:

$$\delta U = \int_L \left(N\delta\varepsilon - M_y \delta k_y - M_z \delta k_z + M_{sv}\delta\theta'_x + B_\omega \delta\theta''_x + \frac{1}{2} M_R \delta(\theta'_x)^2 \right) dx \qquad (7)$$

N is the axial force, M_y and M_z are the bending moments, B_ω is the bimoment acting on the cross-section and M_{sv} is the St-Venant torsion moment (Fig.1). M_R is a higher order stress resultant. It includes Wagner coefficient and shortening effects. Doing variation on relations (1-3), one obtains for the virtual work δW of the external loads:

$$\begin{aligned}
\delta W = {} & \lambda \int_L \left(F_{xe}\delta u + F_{ye}\delta v + F_{ze}\delta w + M_{xe}\delta\theta_x + M_{ye}\delta w' + M_{ze}\delta v' + B_{\omega e}\delta\theta'_x \right) dx \\
& + \lambda \int_L \left(M_{ye}c + M_{ze}s \right)\delta w' \, dS + \lambda \int_L \left(M_{ze}c - M_{ye}s \right)\delta v' \, dx \\
& + \lambda \int_L \left(-F_{ye}\{e_z c + e_y s\} + F_{ze}\{e_y c - e_z s\} - M_{ye}(v' + v'c + w's) + M_{ze}(w' + w'c - v's) \right)\delta\theta_x \, dx
\end{aligned} \qquad (8a)$$

where e_y and e_z denote load eccentricities from shear point ($e_y = y - y_c$, $e_z = z - z_c$), (M_{ye}, M_{ze}), M_{xe} and $B_{\omega e}$ define respectively the external bending moments, the torsion moment and the bimoment. They are listed below in terms of load eccentricities:

$$M_{ye} = -F_{xe}\, z, \quad M_{ze} = -F_{ze}\, y, \quad M_{xe} = -F_{ye}\, e_z + F_{ze}\, e_y, \quad B_{\omega e} = -F_{xe}\, \omega \qquad (8b\text{-}e)$$

In finite element approach, only the contribution of constant load is considered. Distributed loads are converted to equivalent concentrated loads. The contribution of eccentric loads to second member and tangent stiffness matrix is not included in the present work. Extensive effort is done actually in order to make this possible in future with development of an alternative method to Newton-Raphson iterative methods, the asymptotic numeric method [12]. The first results have been already obtained. The results will be presented in near future. When only linear terms are kept in development, the virtual work of external loads is reduced to:

$$\delta W = \lambda \int_L \left(F_{xe}\delta u + F_{ye}\delta v + F_{ze}\delta w + M_{xe}\delta\theta_x + M_{ye}\delta w' + M_{ze}\delta v' + B_{\omega e}\delta\theta_x' \right) dx \tag{9}$$

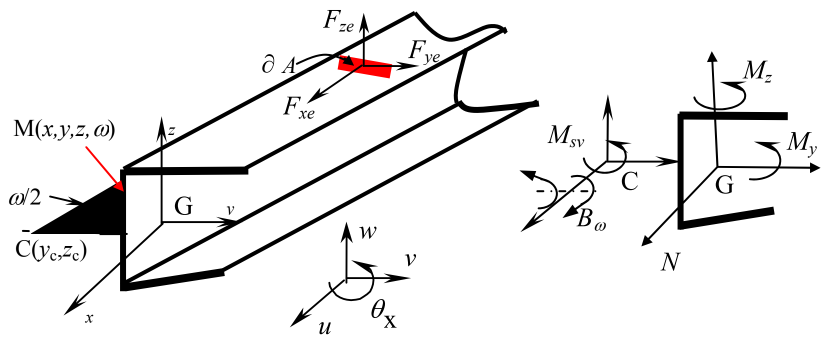

Fig. 1: open section thin-walled beam: definition of kinematics and stress forces

Matrix formulation is adopted hereafter. For the purpose, the following work vectors are introduced:

$$\{S\}^t = \{N \quad M_y \quad M_z \quad M_{sv} \quad B_\omega \quad M_R\}, \qquad \{\gamma\}^t = \left\{\varepsilon \quad -k_y \quad -k_z \quad \theta_x' \quad \theta_x'' \quad \frac{1}{2}\theta_x'^2\right\}$$

$$\{q\}^t = \{u \quad v \quad w \quad \theta_x\}, \qquad \{\theta\}^t = \{u' \quad v' \quad w' \quad \theta_x' \quad v'' \quad w'' \quad \theta_x'' \quad \theta_x\} \tag{10a-d}$$

$$\{F_e\}^t = \{F_{xe} \quad F_{ye} \quad F_{ze} \quad M_{xe}\}, \qquad \{M_e\}^t = \{0 \quad M_{ze} \quad M_{ye} \quad B_{\omega e} \quad 0 \quad 0 \quad 0 \quad 0\} \tag{11a,b}$$

$\{S\}$ and $\{\gamma\}$ define beam stress resultants and deformation vectors. Vectors $\{q\}$ and $\{\theta\}$ are displacement and displacement gradient vectors. Load forces are arranged in two components $\{F_e\}$ and $\{M_e\}$ which are the conjugate of $\{q\}$ and $\{\theta\}$. In previous vectors, the trigonometric functions c and s are present in $\{\gamma\}$ vector, respectively in χ variable of the membrane component ε and in curvatures k_y and k_z defined in (6a-d). For numerical development, the following additional vector is used.

$$\{\alpha\}^t = \{c \quad s \quad \chi\} \tag{12}$$

Based on (10-11), the matrix formulation of the equilibrium in compact form is:

$$\int_L \{\delta\gamma\}^t \{S\} dx - \lambda \left(\int_L \{\delta q\}^t \{F_e\} dx + \int_L \{\delta\theta\}^t \{M_e\} dx \right) = 0 \tag{13}$$

The present model is applied in the case of elastic behaviour. In such context, the matrix form between the stress vector $\{S\}$ and the deformation vector $\{\gamma\}$ when derived in the principal axes is:

$$\{S\} = [D]\{\gamma\} \tag{14}$$

[***D***] is the material matrix behaviour. Its terms are functions on elastic and geometric characteristics needed for axial, bending, and non uniform torsion behaviour [1].

In the variational formulation of the equilibrium (13) and the elastic material behaviour (14), the $\{\gamma\}$ vector and its variation $\{\delta\gamma\}$ are considered particularly since all non linear terms including flexural torsional coupling and trigonometric functions (*c*, *s*) are present in these vectors. According to (6a-c), the strain vector, defined in (10b), is split into a linear part and two non-linear parts:

$$\{\gamma\} = \left([H] + \frac{1}{2}[A(\theta)] - \underline{[A_\alpha(\alpha)]} \right) \{\theta\} \tag{15a}$$

Applying variation to (15a) one gets for $\{\delta\gamma\}$ needed in the equilibrium system (13)

$$\{\delta\gamma\} = \left([H] + [A(\theta)] - \underline{[A_\alpha(\alpha)]} - \underline{[\tilde{A}(\theta,\alpha)]}\right) \{\delta\theta\} \tag{15b}$$

Matrices $[H]$ and $[A(\theta)]$ are classical in non-linear structural mechanics. They are independent on torsion approximation. The terms matrices $[A_\alpha(\alpha)]$ and $[\tilde{A}(\theta,\alpha)]$ that take into account for large torsion and flexural-torsional coupling. For this reason they are outlined. In what follows, only the flexural-torsional matrices are given. The other matrices are detailed in [1]. The $[A_\alpha(\alpha)]$ matrix terms are:

$$[A_\alpha(\alpha)] = \begin{bmatrix} 0 & 0 & 0 & \chi & 0 & 0 & 0 & 0 \\ 0 & 0 & 0 & 0 & -s & c & 0 & 0 \\ 0 & 0 & 0 & 0 & c & s & 0 & 0 \\ 0 & 0 & 0 & 0 & 0 & 0 & 0 & 0 \\ 0 & 0 & 0 & 0 & 0 & 0 & 0 & 0 \\ 0 & 0 & 0 & 0 & 0 & 0 & 0 & 0 \end{bmatrix} \tag{16}$$

For matrix $[\tilde{A}(\theta,\alpha)]$, one gets the following expression:

$$\underline{[\tilde{A}(\theta,\alpha)]} = [\hat{A}(\theta)]\ \underline{[P(\theta,\alpha)]} \tag{17}$$

Matrix $[\hat{A}(\theta)]$ is linearly dependant on $\{\theta\}$. Matrix $[P(\theta,\alpha)]$ is given by:

$$[P(\theta,\alpha)] = \begin{bmatrix} 0 & 0 & 0 & 0 & 0 & 0 & 0 & -s \\ 0 & 0 & 0 & 0 & 0 & 0 & 0 & c+1 \\ 0 & Q_c & R_c & 0 & 0 & 0 & 0 & P_c \end{bmatrix} \tag{18a}$$

$$P_c = -y_c(w's + v'(c+1)) + z_c(v's - w'(c+1))$$

$$Q_c = -y_c s - z_c(c+1) \quad \text{and} \quad R_c = y_c(c+1) - z_c s \tag{18b-d}$$

Based on these relationships, the equilibrium equations (13) and the constitutive system (14) are then arranged into the following detailed system:

$$\begin{cases} \int_L \{\delta\theta\}^t \left([H]+[A(\theta)]-\underline{[A_\alpha(\alpha)]}-\underline{[\tilde{A}(\theta,\alpha)]}\right)^t \{S\}dx - \lambda\left(\int_L \left(\{\delta q\}^t\{F\}+\{\delta\theta\}^t\{M\}\right)dx\right)=0 \\ \{S\}=[D]\left([H]+\frac{1}{2}[A(\theta)]-\underline{[A_\alpha(\alpha)]}\right)\{\theta\} \end{cases} \tag{19a,b}$$

The elastic equilibrium equations have been derived without any assumption about the torsion angle amplitude. Trigonometric functions *c* and *s* have been included as components in vector $\{\alpha\}$. In the analysis, non-linear and highly coupled kinematic relationships have been encountered. Due to consideration of large torsion, novel matrices $[A_\alpha(\alpha)]$ and $[\tilde{A}(\theta,\alpha)]$ derived in terms of functions *c* and *s* and flexural-torsional coupling have been carried out. The finite element approach system (19) is summarised hereafter.

2.2 Finite element formulation and solution strategy

3D beams elements with two nodes and 7 degrees of freedom per node are adopted in mesh process. In the present study, the beam of slenderness *L* is divided into some finite elements of length *l*. Linear shape functions are assumed for axial displacements *u* and cubic functions for the other displacements (i.e *v*, *w*, θ_x) are used. The vectors $\{q\}$ and $\{\theta\}$ are related to nodal variables $\{r\}$ by:

$$\{q\} = [N(\xi)]\{r\}_e \quad \text{and} \quad \{\theta\} = [G(\xi)]\{r\}_e \tag{20a,b}$$

where $[N(\xi)]$ is the shape function matrix and $[G(\xi)]$ is a matrix which links the gradient vector $\{\theta\}$ to nodal displacements. In the framework of finite element method, the system (19) becomes:

$$\begin{cases} \sum_e \frac{l}{2}\int_{-1}^{1}\{\delta r\}_e^t [B(\theta,\alpha)]^t\{S\}d\xi - \lambda\sum_e \frac{l}{2}\int_{-1}^{1}\{\delta r\}_e^t\{f\}_e d\xi = 0 \\ \{S\}=[D]\left([B_l]+\frac{1}{2}[B_{nl}(\theta)]-[B_{nl\alpha}(\alpha)]\right)\{r\}_e \end{cases} \quad \forall\ \{\delta r\} \tag{21a,b}$$

Symbol ($\sum_e$) denotes the assembling process over basic elements. In (21), one reads:

$$[B(\theta,\alpha)]=[B_l]+[B_{nl}(\theta)]-[B_{nl\alpha}(\alpha)]-[\tilde{B}_{nl}(\theta,\alpha)]\ ,$$
$$[B_l] = [H][G(\xi)],$$
$$[B_{nl}(\theta)] = [A(\theta)][G(\xi)],$$
$$[B_{nl\alpha}(\alpha)] = [A_\alpha(\alpha)][G(\xi)]\ ,$$
$$[\tilde{B}_{nl}(\theta,\alpha)] = [\tilde{A}(\theta,\alpha)][G(\xi)],$$

$$\{f\}_e = [N(\xi)]^t\{F_e\} + [G(\xi)]^t\{M_e\} \ . \qquad (22a\text{-}f)$$

Matrices $[B_l]$ and $[B_{nl}(\theta)]$ are familiar in non-linear structural analysis. $[B_{nl\alpha}(\alpha)]$ and $[\tilde{B}_{nl}(\theta,\alpha)]$ result from large torsion assumptions and flexural-torsional coupling. Vector $\{f\}_e$ is related to the nodal forces. To solve the non-linear problem (21) the classical incremental-iterative Newton-Raphson procedure is followed. With this aim in view, we have to compute the tangent stiffness matrix. Unknowns of the problem $(\{U\}^t,\lambda) = (\{r\} \ \{S\} \ \{\alpha\},\lambda)$ are sought in the form:

$$\{U\} = \{U_0\} + \{\Delta U\} \qquad \text{and} \qquad \lambda = \lambda_0 + \Delta\lambda \qquad (23a,b)$$

Given an initial guess of the solution ($\{U_0\}$, λ_0), the increments of the problem ($\{\Delta U\}$, $\Delta\lambda$) fulfil the following incremental condition:

$$[K_t]\{\Delta r\} - \Delta\lambda\{f\} = \{0\} \qquad (24)$$

where: $[K_t] = [K_g] + [K_{s0}]$ (25a)

$$[K_g] = \sum_e \frac{l}{2}\int_{-1}^{1}[B(\theta_0,\alpha_0)]^t[D][B(\theta_0,\alpha_0)]d\xi \qquad (25b)$$

$$[K_{s0}] = \sum_e \frac{l}{2}\int_{-1}^{1}[G(\xi)]^t[S(\theta_0,\alpha_0)][G(\xi)]d\xi \qquad (25c)$$

$[K_t]$ is the tangent stiffness matrix. $[K_g]$ and $[K_{s0}]$ are respectively the geometric and the initial stress stiffness matrices. The geometric matrix terms have been defined previously in (22). The initial stress matrix is split into:

$$[S(\theta_0,\alpha_0] = [\overline{S}_0] - [\overline{\overline{S}}_0(\theta_0,\alpha_0)] - [\overline{\overline{S}}_0(\theta_0,\alpha_0)]^t - [\overline{\overline{\overline{S}}}_0(\theta_0,\alpha_0)] \qquad (26)$$

All these matrices are 8x8 order. The first, ($[\overline{S}_0]$) is function on beam initial stress resultants but is independent to torsion approximation. The last ($[\overline{\overline{S}}_0]$ and $[\overline{\overline{\overline{S}}}_0]$) are highly dependent. The non vanished terms of these matrices are the following:

$$\overline{\overline{S}}_0(4,2) = N_0 Q_c, \qquad \overline{\overline{S}}_0(4,3) = N_0 R_c, \qquad \overline{\overline{S}}_0(4,8) = N_0 P_c,$$

$$\overline{\overline{S}}_0(5,8) = -M_{z0}s - M_{y0}(c+1), \qquad \overline{\overline{S}}_0(5,8) = -M_{y0}s + M_{z0}(c+1) \qquad (27a\text{-}e)$$

$$\overline{\overline{\overline{S}}}_0(2,8) = -N_0\theta_x^{'}(y_c(c+1) - z_c s) \qquad \overline{\overline{\overline{S}}}_0(2,8) = -N_0\theta_x^{'}(y_c s + z_c(c+1))$$

$$\begin{aligned}\overline{\overline{\overline{S}}}_0(8,8) &= N_0\theta_x^{'}[y_c(v's - w'(c+1)) + z_c(v'(c+1) + w's)] \\ &+ M_{y0}[v''s - w''(c+1)] - M_{z0}[w''s + v''(c+1)]\end{aligned} \qquad (28a\text{-}c)$$

In these relationships, N_0, M_{y0} and M_{z0} are axial and bending initial beam stress resultants. Coefficients P_c, Q_c and R_c have been defined in (18b-d).

By this way, a large torsion non-linear finite element model for elastic thin-walled beams has been investigated. The calculation of the tangent stiffness matrix was possible thanks to the introduction of trigonometric variables c and s present in $\{\alpha\}$ vector. The different solutions are first presented and discussed below.

3 Finite element formulations with polynomial approximations

In previous formulation, all matrices are derived without any assumption on torsion angle amplitudes. Functions $c=cos(\theta_x)$-1 and $s= sin(\theta_x)$ have been considered without any approximations. In what follows, these functions are computed according to the following Taylor's approximants, ranging from cubic to linear.

When functions c and s are approximated until power 3 (cubic approximation), then:

$$\cos(\theta_x) = 1 - \frac{\theta_x^2}{2}, \quad \sin(\theta_x) = \theta_x - \frac{\theta_x^3}{6}, \qquad \text{so:} \quad c = -\frac{\theta_x^2}{2}, \qquad s = \theta_x - \frac{\theta_x^3}{6} \qquad \text{(29a-d)}$$

The kinematics (1-3) of displacement components are modified accordingly.

$$\begin{aligned} u_M &= u - y\left(v'(1-\frac{\theta_x^2}{2}) + w'(\theta_x - \frac{\theta_x^3}{6}) \right) - z\left(w'(1-\frac{\theta_x^2}{2}) - v'(\theta_x - \frac{\theta_x^3}{6}) \right) - \omega\theta_x' \\ v_M &= v - (z - z_c)(\theta_x - \frac{\theta_x^3}{6}) - (y - y_c)\frac{\theta_x^2}{2} \\ w_M &= w + (y - y_c)(\theta_x - \frac{\theta_x^3}{6}) - (z - z_c)\frac{\theta_x^2}{2} \end{aligned} \qquad \text{(30a-c)}$$

When functions c and s are approximated until power 2 (quadratic), one writes:

$$\cos(\theta_x) = 1 - \frac{\theta_x^2}{2}, \sin(\theta_x) = \theta_x, \quad c = -\frac{\theta_x^2}{2} \text{ and } \quad s = \theta_x \qquad \text{(31a-d)}$$

The 3D displacements of the beam's contour point are:

$$\begin{aligned} u_M &= u - y\left(v'(1-\frac{\theta_x^2}{2}) + w'\theta_x \right) - z\left(w'(1-\frac{\theta_x^2}{2}) - v'\theta_x \right) - \omega\theta_x' \\ v_M &= v - (z - z_c)\theta_x - (y - y_c)\frac{\theta_x^2}{2} \\ w_M &= w + (y - y_c)\theta_x - (z - z_c)\frac{\theta_x^2}{2} \end{aligned} \qquad \text{(32a-c)}$$

When the functions c and s are approximated with only linear functions, one gets:

$$\cos(\theta_x) = 1, \qquad \sin(\theta_x) = \theta_x \quad, \qquad c = 0 \quad, \qquad s = \theta_x \qquad \text{(33a-d)}$$

This means, that in kinematic equations, one considers:

$$u_M = u - y(v' + w'\theta_x) - z(w' - v'\theta_x) - \omega\theta_x'$$
$$v_M = v - (z - z_c)\theta_x \quad , \quad w_M = w + (y - y_c)\theta_x \qquad \text{(34a-c)}$$

For these approximations, the same procedure is followed as in large torsion context. For any approximation, the equilibrium system and its finite element formulation are derived. For the equilibrium, the matrix formulation equivalent to (19) is obtained. Changes are observed at matrices linked to flexural-torsional coupling (i.e: matrices $[A_\alpha(\alpha)]$, $[P(\theta,\alpha)]$). In solution of the nonlinear equations by iterative incremental strategies, the initial stress matrices $\left[\overline{\overline{S}}(\theta_0,\alpha_0)\right]$ and $\left[\overline{\overline{\overline{S}}}(\theta_0,\alpha_0)\right]$ of the tangent operator $[K_t]$ are carried out. Their terms are derived in the Appendix **A** for any approximation and a finite element model based on 3D beam element including warping and according to each previous approximation has been developed. Due to highly coupled and non linear equilibrium equations, the Newton-Raphson incremental iterative methods are adopted in the solution. Here, the arc-length strategy is adopted. The tangent matrix is then carried out. It accounts for large displacements, initial stresses, torsion approximation and flexural-torsional coupling. These elements are implanted in a general finite element package. The large torsion beam element referenced B3Dw has been presented largely and validated in [1]. The beam elements are denoted B3Dw3 (for cubic approximation), B3Dw2 (quadratic approximation) and B3Dw1 (linear approximation). Some examples are presented hereafter. They concern the flexural-torsional behaviour of beams under torsion moment and post buckling behaviour of columns and beams.

4 Comparison examples

Some comparison examples are considered here. They concern non linear behaviour of beams with arbitrary cross section under twist moment and post buckling behaviour of columns and beams under axial loads or bending loads. Due to presence of highly non linear equations and presence of singular points, arc-length method is adopted for solution of the incremental equations. For each element, the flexural-torsional equilibrium paths are obtained under the same conditions (mesh, initial arc-length increment, convergence criteria and initial imperfections when they are needed).

4.1 Torsion behaviour

The flexural torsional behaviour of a channel beem under torsion moment is studied. The beam is simply supported in bending and torsion at both ends. Warping is free at both ends. The axial displacement is fixed only at one end. The geometric data of the beam are depicted in Fig.2a. The elastic constants E=210 GPa G=80,77 GPa. A torsion moment is applied at mid-length. 20 elements are used in the mesh process.

Since the beam cross section is singly symmetric, it exhibits a flexural-torsional beahviour. The displacements v,w and the torsion angle θ_x at mid-length of the beam are depicted in Fig.2b-d. The torsion moment has been varied from 1 to 100 kNm with an automatic arc-length. For the convergence condition, the residue is fixed at 10^{-6}. One can observe that in large torsion beam behaviour of the beam is predominated by shortening effect. For this section the linear part is very limited. Effect of torsion approximation is evident. Under linear behaviour assumption, one observe that torsion angle increase continuously with the applied moment. With B3Dw elements, amplitudes of dipslacements (v and w) are bounded in positive and negative values. The polynomial approximations from cubic, quadratic and linear are valid near the origin where the torsion angle is less than 1.0 rad ($M_x \leq 10kNm$). They are not able to follow B3Dw predictions far from the origin.

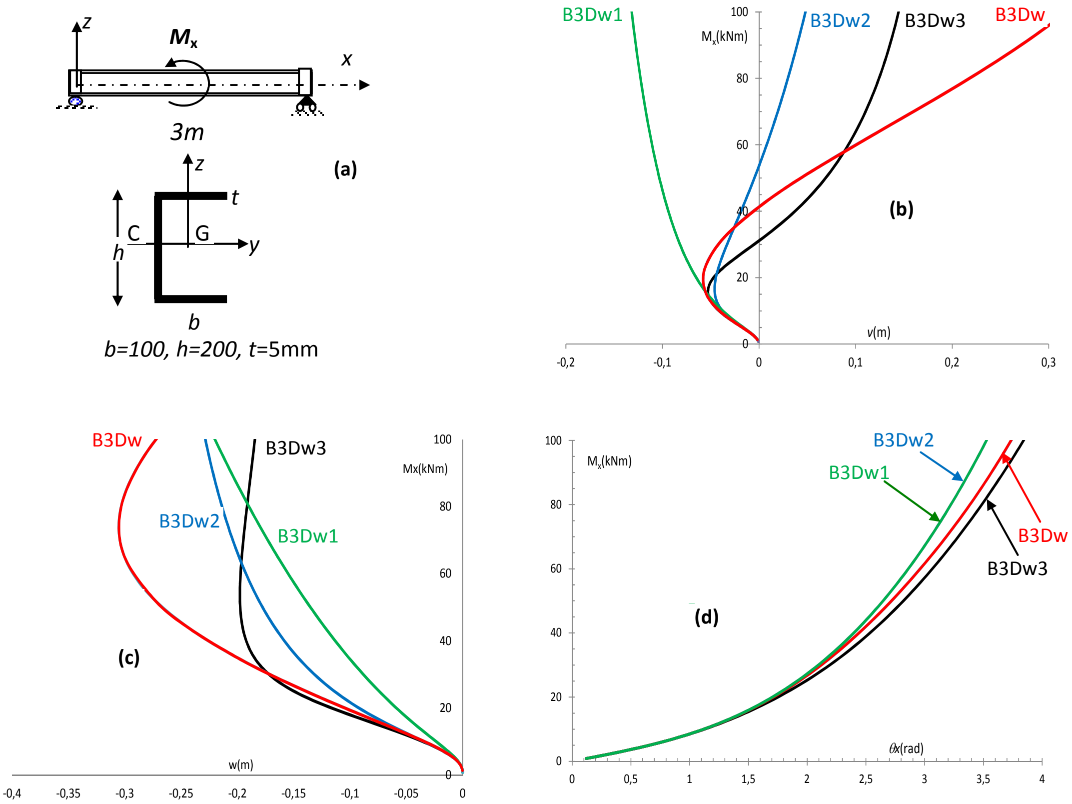

Fig.2: Flexural-torsional behaviour of a beam under torsion moment
(a): data, (b): (M_x,v) curve, (c): (M_x,w) curve, (d): torsion behaviour.

4.2 Post buckling analysis of channel section in compression

The previous steel beam with channel cross section is studied now under compressive load (λF_x). In order to reach the post buckling equilibrium curves, initial additional loads (λM_x λF_z) are applied. In the analysis, F_x is fixed to 1 kN and the imperfection loads (F_z M_x) are very small, fixed to 0.01. The flexural-torsional equilibrium curves are depicted in Figs.3b-d. One can observe that the buckling load is independent to torsion approximation. Its value is **366.7 kN**. The equilibrium curves are instable near buckling load. With B3Dw a looping curve is present in (P,v). Near buckling load area, cubic element B3Dw3 follow the decrease part but it is not able to describe the perfectly the looping curve. B3Dw2 and B3Dw1 elements lead to flat and stiff curves. Limits of these approximations in post buckling analyses, far from bifurcation zone are then evident.

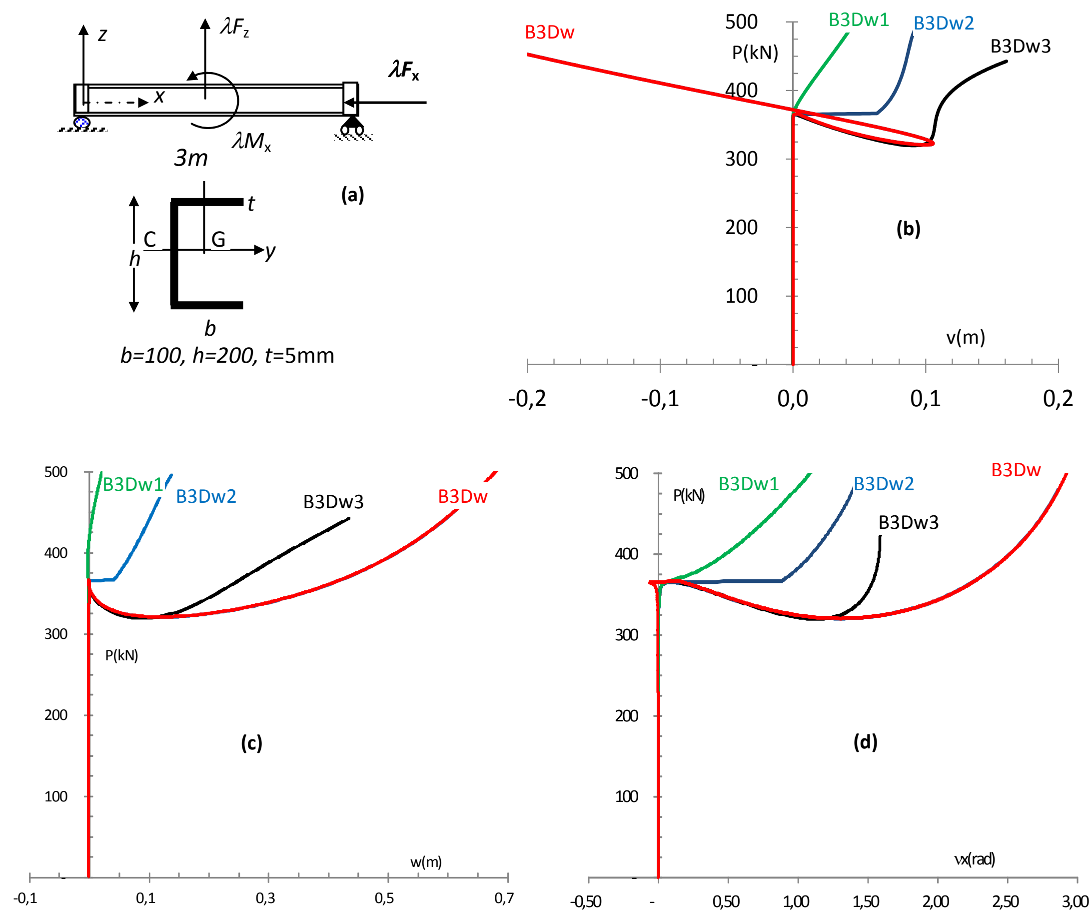

Fig.3: Post-buckling behaviour of a beam under compression
(a): data, (b): (P,v) curve, (c): (P,w) curve, (d): (P,θ_x) curve

4.3 Lateral post buckling analysis of I beam

An European steel beam with I300 cross section (b=150,h=300,t_f=10,7,t_w=6,1mm) is considered. The beam, of length L=6m, is subjected at mid length to a concentrated load ($\boldsymbol{\lambda Q_z}$). In order to reach the post buckling equilibrium curves, initial additional loads ($\lambda F_y,\lambda M_x$) are applied. In the analysis, Q_z is fixed to 1 kN and imperfection loads F_y and M_x to 0.01. The flexural-torsional equilibrium curves are depicted in fig.4a-c. These curves are obtained with an automatic arc length varying load until 500 kN. One can observe that the buckling load is independent to torsion approximation. Its value is 78 kN. The displacement v is bounded and don't increase in post buckling state. Cubic element B3Dw3 is slightly different than B3dw predictions. B3Dw2 and B3Dw1 elements lead to continuously stiff curves. Limits of these approximations in post buckling analyses are then evident.

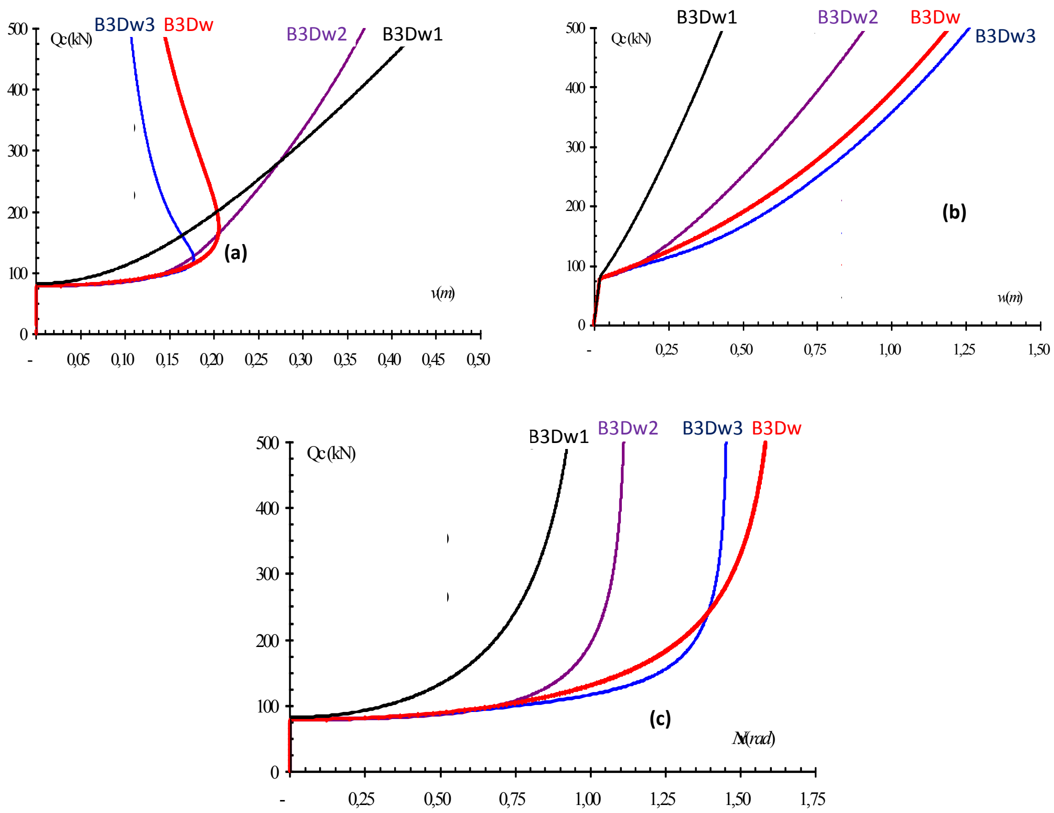

Fig.4: lateral post-buckling behaviour of a beam
(a): (P,v) curve, (b): (P,w) curve, (c): (P,θ_x) curve

4.4 Lateral buckling stability of continuous beams

In order to demonstrate the efficiency of the B3Dw, it is important to consider cases when boundary conditions are arbitrary. The last example is devoted to lateral buckling of continuous beam ABC with two equal spans under two centrally loads Q_1 and Q_2 applied at each span at point M_1 and M_2. The beam is under simply supported boundary conditions in bending and torsion at ends A, B and C. The warping is free at each beam end and continuous at the central support B. The axial displacement is restrained only at support A. This example has been studied by Vachagitiphan [13], where a doubly-symmetric steel I-section called UC31 is used. Pre-buckling deflection effect on beam lateral buckling resistance is studied by varying load factors of Q_1 and Q_2 from zero to unity. In numerical approach, buckling loads are obtained according to eigenvalue problem solutions (EVP) and non linear bifurcations detected along the beam equilibrium curves (B3Dw). In order to reach post-buckling range, some initial flexural-torsional imperfections have been considered at points M_1 and M_2. The buckling interaction curves are depicted in Fig. 5. This section is very sensitive to pre-buckling deflections. Buckling loads carried out from EVP solutions underestimate thremousthly beam resistance against lateral buckling for all load intensities. When Q_1 and Q_2 have different intensities the beam deformation is not symmetric. But when their intensities are close (Q_1=Q_2) symmetric and anti-symmetric modes are possible. Buckling loads are derived for the Anti-symmetric Mode (AM) and Symmetric Mode (SM) from EVP approach and nonlinear analysis.

- For the AM, the EVP gives the buckling load (Q_1=Q_2=212 kN). Based on nonlinear analysis approach, these loads increase to (Q_1=Q_2=265 kN). Fig. 6a,b depict the post buckling curves of the deflection and torsion angles at points M_1 and M_2 related to this mode.
- For the SM, the EVP leads the buckling load (Q_1=Q_2=279 kN). In nonlinear analysis, these loads reach value (Q_1=Q_2=339 kN). The related post buckling curves (Q,w) and (Q,θ_x) at points M_1 and M_2 are pictured in figs 6c,d.
- In Vachagitiphan [13], only the interaction curve of AM was depicted. The agreement is very good.

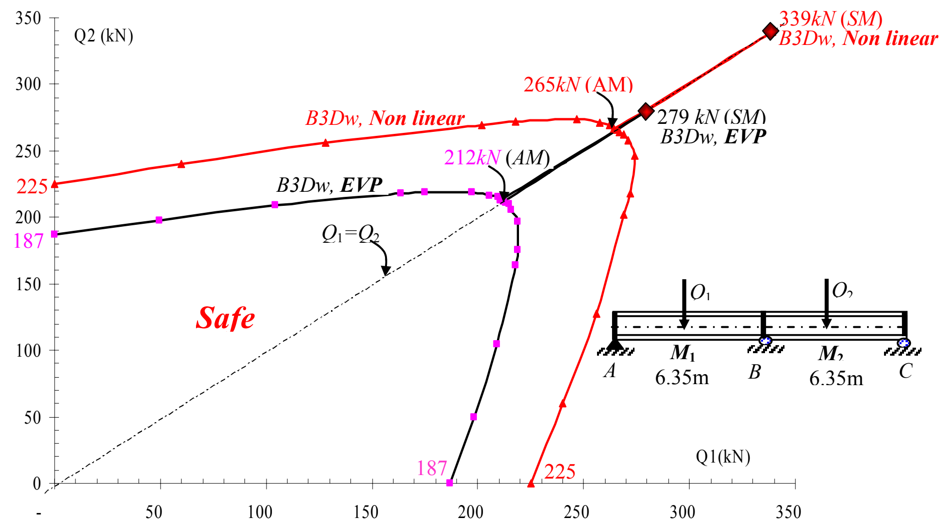

Fig.5: Buckling load interaction curve for two span continuous I-beam
(SM: buckling load with symmetric mode, AM: buckling load with anti-symmetric mode)

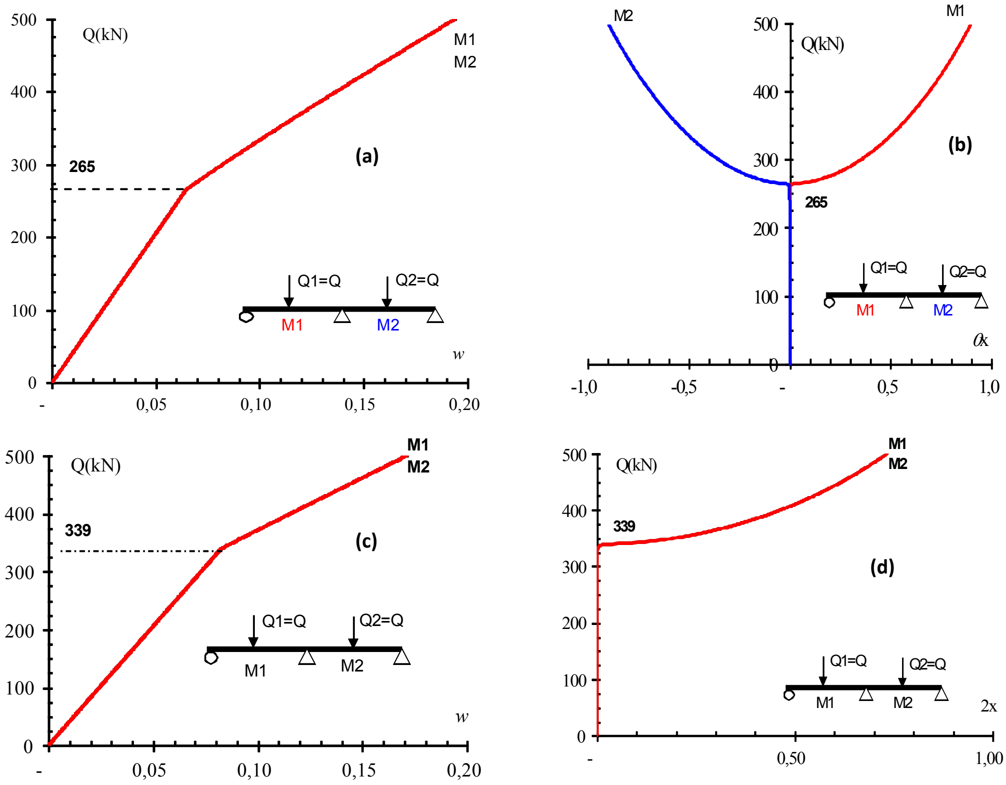

Fig.6: Post buckling equilibrium curves of points M_1 and M_2: (a) deflection (AM), (b) torsion (AM), (c) deflection (SM), (d) torsion (SM).

5 Conclusions

Four beam finite elements have been investigated for thin-walled elements. They use three-dimensional beams with two nodes and seven degrees of freedom (dof) per node. Warping is considered as independent degree of freedom. In the first (B3dw), trigonometric functions c=cos θ_x-1 and s=sin θ_x are used in the whole model without any approximation. The equilibrium equations are derived in discrete form. For non linear behaviour, the tangent stiffness matrix is carried out in terms of large displacements and initial stresses. The tree others elements are derived with polynomial functions for the trigonometric functions c and s: cubic (B3Dw3), quadratic (B3Dw2) and linear approximation (B3Dw1). The same procedure has been followed in the equilibrium, discretization and derivation of the tangent operator. The matrices which are function on flexural-torsional coupling and torsion approximation are derived for the equilibrium and tangent operator. Many comparison examples have been considered. They concern non linear behaviour of beams with arbitrary cross section under twist moment and post buckling behaviour of columns and beams under axial loads or bending loads. For each studied case, the flexural-torsional equilibrium paths are obtained under the same conditions. The efficiency of B3Dw element is confirmed from benchmark solutions. From the equilibrium curves obtained with the other elements, it is concluded that:

1. For the torsion behaviour, the accuracy is function on approximation. B3Dw3 is more accurate than B3Dw2 and B3Dw1 which become inadequate or fail when torsion angles become finite or large.
2. In stability analyses, the buckling loads of beams under axial or lateral loads are independent to torsion approximation. All elements lead to the same buckling loads with the same accuracy.
3. In post buckling behaviour, the equilibrium curves of B3Dw1 and B3Dw2 elements are valid only in regions near bifurcation. B3Dw3 is accurate until moderate torsion angles are reached.
4. B3Dw is reconsidered for the lateral buckling stability of two span continuous beams under two centrally concentrated loads. The interaction curve is carried out. It is observed that buckling modes are anti symmetric when intensity loads is different. Under equal loads symmetric and anti symmetric are possible.

In this paper, only a constant load contribution is considered in the finite element procedure. The effect of non constant load effects has not been included in the finite element model. This part will contribute to the right hand side and to the tangent stiffness matrix. By this way, the load application from shear point and centroid will be taken into account. This work is now in good progress with application of the asymptotic numerical method [12]. The results will be presented in the near future.

References

[1] Mohri F, Damil N and Potier-Ferry M (2008) *Large torsion finite element model for thin-walled beams.* Computers and Structures, 86, 671-683.

[2] Bazant, ZP, El Nimeiri M *Large-deflection spatial buckling of thin walled beams and frames.* Journal of Engineering Mechanics Division, 99, 1259-1281, 1973

[3] Laudiero F, Zaccaria D (1988) *Finite Element Analysis of stability of thin-walled beams of open section*. Int. Journal of Mechanical Sciences, 30, 543-557

[4] Pi YL, Bradford MA *Effects of approximations in analyses of beams of open thin-walled cross-section. Part II:* 3-*D non-linear behaviour.* International Journal for Numerical Method in Engineering, 51, 773-790, 2001

[5] Turkalj G, Brnic J and Prpic-Orsic J. *Large rotation analysis of elastic thin-walled beam-type structures using ESA approach.* Computers and Structures, 81, 1851-1864, 2003

[6] Attard MM *Lateral buckling analysis of beams by the FEM*, Computers and Structures, 23, 217-231, 1986

[7] Ronagh HR, Bradford MA, Attard MM *Nonlinear analysis of thin-walled members of variable cross-section,* Computers and Structures, 77 301-313, 2000

[8] Mohri F, Azrar L and Potier-Ferry M *Flexural-torsional post-buckling analysis of thin-walled elements with open sections*. Thin-Walled Structures 39, 907-938, 2001
[9] Sapountzakis E J Dourakopoulos JA *Flexural–torsional postbuckling analysis of beams of arbitrary cross section*. Acta Mech 209, 67-84, 2010
[10] De Ville de Goyet V *L'analyse statique non linéaire des structures spatiales formées de poutres à sections non symétrique par la méthode des éléments finis*. PHD Thesis. University of Liege, Belgium, 1989
[11] Fraternali F, Feo L *On a moderate rotation theory of thin-walled composite beams Composites: Part B*, 31, 141–158, 2000
[12] Cochelin B, Damil N, Potier-Ferry M *Méthode Asymptotique Numérique.* Hermès, Paris. 2007
[13] Vachagitiphan P, Woolcock ST, Trahair NS "*Effect of in-plane deformation on lateral buckling*". Journal of structural mechanics, ASCE, 3(11), 29–60.1974

Appendix A: Flexural torsional matrix terms according to different approximations

A.1 Equilibrium system

For this approximation, the equilibrium system is carried as followed in large torsion. Equivalent system as (19) is obtained. Changes are observed at matrices linked to flexural-torsional coupling (matrices terms $[A_\alpha(\alpha)]$ $[P(\theta,\alpha)]$). The non vanished terms of these matrices are:

A.1.1 Cubic approximation

Matrix $[A_\alpha(\theta,\alpha)]$ terms:

$$A_\alpha(1,4)=y_c\left(w'(1-\frac{\theta_x^2}{2})-v'(\theta_x-\frac{\theta_x^3}{6}\right)-z_c\left(v'(1-\frac{\theta_x^2}{2})+w'(\theta_x-\frac{\theta_x^3}{6})\right)$$

$$A_\alpha(2,5)=-(\theta_x-\frac{\theta_x^3}{6}) \qquad A_\alpha(2,6)=-\frac{\theta_x^2}{2}$$

$$A_\alpha(3,5)=-\frac{\theta_x^2}{2} \qquad A_\alpha(3,6)=(\theta_x-\frac{\theta_x^3}{6})$$

Matrix $[P(\theta,\alpha)]$ terms:

$$P(1,8)=-\theta_x \qquad P(2,8)=-\left(1-\frac{\theta_x^2}{2}\right), \qquad P(3,2)=-\left(y_c(\theta_x-\frac{\theta_x^3}{6})+z_c(1-\frac{\theta_x^2}{2})\right)$$

$$P(3,2)=y_c(1-\frac{\theta_x^2}{2})-z_c(\theta_x-\frac{\theta_x^3}{6}), \qquad P(3,8)=-y_c\left(w'\theta_x+v'(1-\frac{\theta_x^2}{2})\right)+z_c\left(v'\theta_x-w'(1-\frac{\theta_x^2}{2})\right)$$

A.1.2 Quadratic approximation

Matrix $[A_\alpha(\theta,\alpha)]$ terms:

$$A_\alpha(1,4) = y_c\left(w'(1-\frac{\theta_x^2}{2}) - v'\theta_x\right) - z_c\left(v'(1-\frac{\theta_x^2}{2}) + w'\theta_x\right)$$

$$A_\alpha(2,5) = -(\theta_x - \frac{\theta_x^3}{6}) \qquad A_\alpha(2,6) = -\frac{\theta_x^2}{2}$$

$$A_\alpha(3,5) = -\frac{\theta_x^2}{2} \qquad A_\alpha(3,6) = (\theta_x - \frac{\theta_x^3}{6})$$

Matrix $[P(\theta,\alpha)]$ terms

$$P(1,8) = -\theta_x \qquad P(2,8) = 1$$

$$P(3,2) = -\left(y_c\theta_x + z_c(1-\frac{\theta_x^2}{2})\right), \qquad P(3,3) = y_c(1-\frac{\theta_x^2}{2}) - z_c\theta_x$$

$$P(3,8) = -y_c(w'\theta_x + v') + z_c(v'\theta_x - w')$$

A.1.3 Linear approximation

Here the formulation is less different than in the precedent approximations. In the equilibrium equations, the coupling is not strong. One arrives to:

$$\begin{cases} \int_L \{\delta\theta\}^t \left([H] + [A(\theta)] - \underline{[A_\alpha(\theta)]} - \underline{[\tilde{A}(\theta)]}\right)^t \{S\}dx - \lambda\left(\int_L \left(\{\delta q\}^t\{F\} + \{\delta\theta\}^t\{M\}\right)dx\right) = 0 \\ \{S\} = [D]\left([H] + \frac{1}{2}[A(\theta)] - \underline{[A_\alpha(\theta)]}\right)\{\theta\} \end{cases}$$

$$A_\alpha(1,4) = y_c w' - z_c v', \quad A_\alpha(2,5) = -\theta_x$$

$$A_\alpha(3,6) = \theta_x, \qquad \tilde{A}(1,2) = -z_c\theta_x'$$

$$\tilde{A}(1,3) = y_c\theta_x', \qquad \tilde{A}(2,8) = -v'', \qquad \tilde{A}(3,8) = w''$$

A.2 Initial stress matrices terms

A.2.1 Cubic approximation

The equilibrium system is nonlinear and highly coupled. The Newton-Raphson iterative method is adopted is solution procedure. The tangent operator is then derived. The initial stress matrices due to flexural-torsional coupling needed in solution $\left[\overline{\overline{S}}\right]$ and $\left[\overline{\overline{\overline{S}}}\right]$ terms have the following expressions.

$$\overline{\overline{S}}_0(4,2) = -N_0\left(y_c(\theta_x - \frac{\theta_x^3}{6}) + z_c(1-\frac{\theta_x^2}{2})\right)$$
$$\overline{\overline{S}}_0(4,3) = N_0\left(y_c(1-\frac{\theta_x^2}{2}) - z_c(\theta_x - \frac{\theta_x^3}{6})\right)$$
$$\overline{\overline{S}}_0(4,8) = N_0\left\{ - y_c\left(w'\theta_x + v'(1-\frac{\theta_x^2}{2})\right) + z_c\left(v'\theta_x - w'(1-\frac{\theta_x^2}{2})\right)\right\}$$
$$\overline{\overline{S}}_0(5,8) = -M_{z0}\theta_{x0} - M_{y0}(1-\frac{\theta_{x0}^2}{2}) \qquad \overline{\overline{S}}_0(6,8) = -M_{y0}\theta_{x0} + M_{z0}(1-\frac{\theta_{x0}^2}{2})$$
$$\overline{\overline{\overline{S}}}_0(2,8) = \overline{\overline{\overline{S}}}_0(8,2) = -N_0\theta_x^{'}\left(y_c(1-\frac{\theta_x^2}{2}) - z_c\theta_x\right)$$
$$\overline{\overline{\overline{S}}}_0(3,8) = \overline{\overline{\overline{S}}}_0(8,3) = -N_0\theta_x^{'}\left(y_c\theta_x + z_c(1-\frac{\theta_x^2}{2})\right)$$
$$\overline{\overline{\overline{S}}}_0(8,8) = N_0\theta_x^{'}\left[y_c\left(v^{'}\theta_x - w'\right) + z_c\left(v^{'} + w'\theta_x\right)\right] + M_{y0}\left(v''\theta_x - w''\right) - M_{z0}\left(w''\theta_x + v''\right)$$

A.2.2 Quadratic approximation

The initial stress matrices $\left[\overline{\overline{S}}\right]$ and $\left[\overline{\overline{\overline{S}}}\right]$ terms are:

$$\overline{\overline{S}}_0(4,2) = -N_0\left(y_c\theta_x + z_c(1-\frac{\theta_x^2}{2})\right) \qquad \overline{\overline{S}}_0(4,3) = N_0\left(y_c(1-\frac{\theta_x^2}{2}) - z_c\theta_x\right)$$
$$\overline{\overline{S}}_0(4,8) = N_0\left(- y_c(w'\theta_x + v') + z_c(v'\theta_x - w')\right)$$
$$\overline{\overline{S}}_0(5,8) = -M_{z0}\theta_{x0} - M_{y0}$$
$$\overline{\overline{S}}_0(6,8) = -M_{y0}\theta_{x0} + M_{z0}$$

$$\overline{\overline{\overline{S}}}_0(2,8) = \overline{\overline{\overline{S}}}_0(8,2) = -N_0\theta_x^{'}\left(y_c - z_c\theta_x\right) \qquad \overline{\overline{\overline{S}}}_0(3,8) = \overline{\overline{\overline{S}}}_0(8,3) = -N_0\theta_x^{'}\left(y_c\theta_x + z_c\right)$$
$$\overline{\overline{\overline{S}}}_0(8,8) = N_0\theta_x^{'}\left[- y_c w' + z_c v'\right] - M_{y0}w'' - M_{z0}v''$$

A.2.3 Linear approximation

Here the formulation is less different than in the precedent approximations. In the equilibrium equations, the coupling is not strong. The initial stress stiffness matrix is given by:

$$\left[S_0\right] = \left[\overline{S}_0\right] - \left[\overline{\overline{S}}_0\right] - \left[\overline{\overline{S}}_0\right]$$

Here the matrix $\left[\overline{\overline{S}}\right]$ is constant and depend only on beam initial stresses. The non vanished terms of this matrix are.

$\overline{\overline{S}}_0(4,2) = -N_0 z_c$ $\qquad$ $\overline{\overline{S}}_0(4,3) = N_0 y_c$

$\overline{\overline{S}}_0(4,8) = -M_{y0}$ $\qquad$ $\overline{\overline{S}}_0(5,8) = M_{z0}$

Matrix $\left[\overline{\overline{\overline{S}}}\right]$ is not present**.**